

## Atomic-Resolution Imaging of Calcite Dissolution Processes by High-Speed Atomic Force Microscopy

\*Takeshi Fukuma<sup>1</sup>

1.Kanazawa University

Calcium carbonates play critical roles in the global carbon cycle and thereby influence the Earth's aerial, aquatic and geologic environments. Calcite is among the most abundant and reactive mineral and hence its crystal growth and dissolution are important. In particular, the calcite dissolution has attracted growing interests due to the recent efforts in geologic carbon sequestration: the storage of carbon dioxide into the subsurface, as it may form leakage paths for the stored carbon. To accurately simulate such long-term and large-scale carbon cycles, it is important to understand the mechanism and kinetics of the calcite dissolution processes.

So far, calcite dissolution processes have been investigated by various methods. The macroscopic behavior has been investigated by monitoring changes in the ion concentration in the solution during the dissolution processes. The nanoscale behavior has been studied by imaging real-time and real-space movements of the single atomic steps by atomic force microscopy (AFM) or optical measurement techniques. However, the establishment of the atomic-scale crystal dissolution model requires understanding of the atomic-scale behavior near the step edges. However, conventional measurement techniques do not allow to directly image such behavior with sufficient spatial and temporal resolution.

Frequency modulation atomic force microscopy (FM-AFM) has traditionally been used for atomic- or molecular-scale investigations on the surface structures and properties of various materials in ultrahigh vacuum. In 2005, we enabled to operate FM-AFM in liquid with true atomic resolution. Furthermore, we recently improved its imaging speed from ~1 frame/min to ~1 frame/sec without losing its high spatial resolution. With the developed high-speed FM-AFM, we succeeded in imaging calcite dissolution processes with atomic-scale resolution. The results reveal the existence of a transition region with a width of 1-8 nm near the step edges. Although the origin of the transition region is still under investigation, this finding should greatly improve our understanding on the atomic-scale behavior of calcite crystal dissolution processes. The results opens up broad range of future applications of the high-speed FM-AFM on crystal growth and dissolution processes.

Keywords: Atomic Force Microscopy, Calcite, Crystal Dissolution

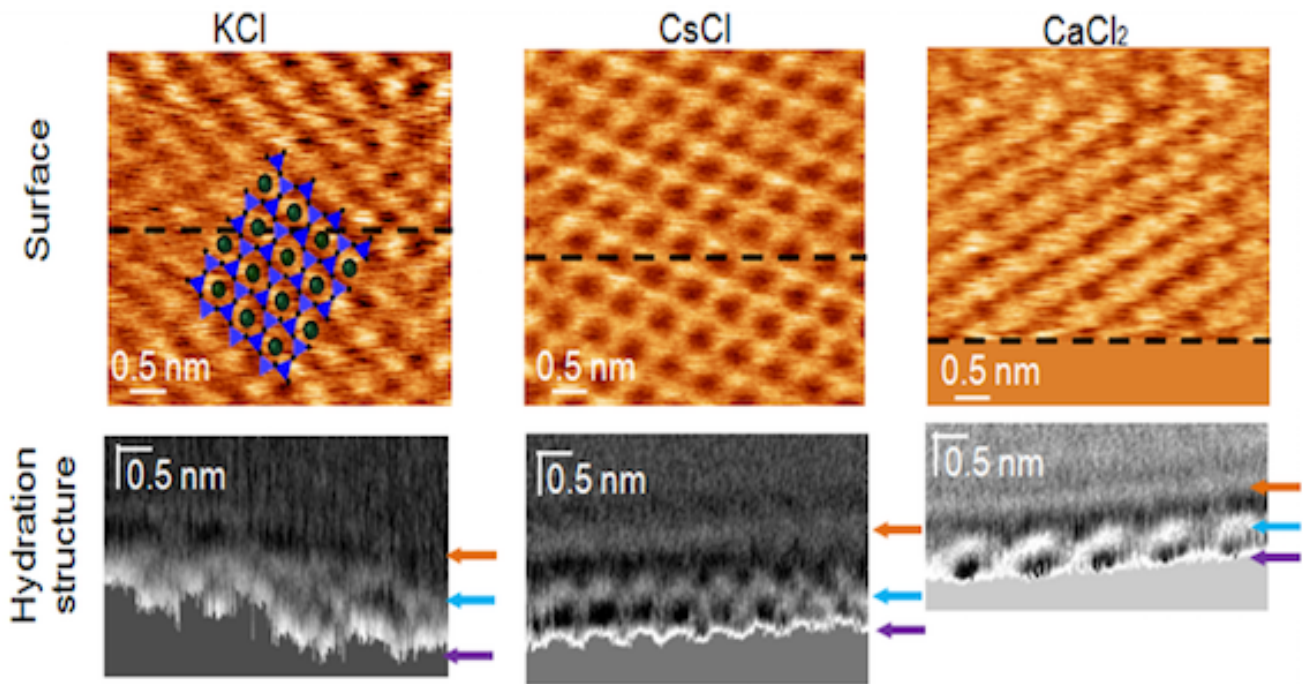
## Dependence of ion exchange on the hydration structure of montmorillonite surfaces probed by atomic-scale observation of solid-liquid interface

\*Yuki Araki<sup>1</sup>, Hisao Satoh<sup>2</sup>, Hiroshi Onishi<sup>1</sup>

1.Graduate School of Science, Kobe University, 2.Mitsubishi Materials Corporation

Cations of clay mineral are exchangeable depending on the atomic weight and electric density. Because of this ion exchange property, the clays are expected to capture the radionuclide which is diffused in the soil. Recently, the effect of water molecules on the ion exchange tendency has been suggested (S. Charles et al., 2006). In order to clarify the behavior of the water molecules at the clay-solution interface, we conducted the atomic-scale observation of the hydration structure in the vicinity of the montmorillonite surfaces in several ionic solutions. The frequency modulation atomic force microscopy (FM-AFM) which was modified based on the commercial AFM (SPM-9600, Shimadzu Corp., Japan) was employed for the atomic scale observation of interfacial structure (T. Fukuma et al., 2005). This FM-AFM technique has achieved the visualization of the 2D or 3D density map of the water molecules in the vicinity of crystal surfaces (K. Kimura et al., 2010; T. Fukuma et al., 2010). We observed the natural montmorillonite surfaces by FM-AFM in the 0.1 M KCl, CsCl, CaCl<sub>2</sub> solutions, respectively. The 100 nm plate-like particles of the montmorillonite were fixed on the mica substrate surfaces, then the (001) face and the interface were observed (Fig.1). The upper images in Fig.1 show the topography of the montmorillonite surfaces. The protrusions (brighter areas) indicate the cation sites of the montmorillonite surfaces which were located in the center of the six-membered rings of silicate tetrahedra. The interface of the montmorillonite and the solutions were observed along the dashed line in the upper images (bottom images in Fig.1). The bottom images showed the three brighter layers presented by arrows. These brighter areas indicate the distribution of the hydrated water molecules. Our results revealed that the hydration structure in the vicinity of the montmorillonite surfaces is uniform regardless of the cations in the solutions. It is suggested that the water molecules around the surface would not affect the ion exchange at the clay surfaces.

Keywords: clay mineral, ion exchange, hydration, frequency modulation AFM (FM-AFM)



## Euler angle calculation and evaluation for orientation indexing of Electron Backscatter Diffraction(EBSD)

\*hirobumi morita<sup>1</sup>, Jenny Goulden<sup>2</sup>

1.Oxford Instruments KK, 2.Oxford Instruments Nanaoanalysis

Recently Electron Backscatter Diffraction (EBSD) with Scanning Electron Microscope (SEM) is applied to geological science, which is also called SEM-EBSD method. There has been a plenty of application results of cubic crystal systems in metallurgy field. But the lower symmetry crystal system such as 180 degrees symmetry is more interested in wide variety of field, e.g. metallurgy, semiconductor, geology and also in more complicated materials. Those crystal system examples are hexagonal, tetragonal, etc.

EBSD identifies Kikuchi pattern and indexes the orientation. As of symmetry of Kikuchi pattern, some orientation and measurement condition cannot index the orientation right in a single solution, having pseudo-symmetric plurality. The sample has to be tilted 70 degrees. Tilt direction, detector to sample orientation, SEM scanning direction, etc. affect the orientation determination significantly. Three dimensional orientations are defined as following Bunge convention <sup>[1][2][3]</sup>. But Euler angle calculated from Kikuchi pattern often changes with the acquisition coordinate system. I would introduce each acquisition coordinate system and Euler angle results and how to interpret the Euler angle results, specifically for hexagonal and tetragonal crystal systems.

### Reference

1. Randle, V., and Engler, O., Texture Analysis, Macrotecture, Microtexture and Orientation Mapping, Taylor and Francis, 2000, ISBN 9056992244
2. Bunge, H.J. 1982. Texture Analysis in Materials Science -Mathematical Methods. Butterworths, London.
3. Bunge, 1993, Texture Analysis in Materials Science, ISBN 3-928815-18-4)

Keywords: Euler angle, EBSD



Fig.1 detector to sample direction

## Direct observation of metastable phase in protein crystallization using transmission electron microscopy

\*Tomoya Yamazaki<sup>1</sup>, Yuki Kimura<sup>1</sup>

1. Institute of Low Temperature Science Hokkaido University

A thermodynamically metastable phase, such as amorphous and dense liquid, has an important role in a crystallization process. In a nucleation process, amorphous particles appear before nucleation of a crystalline phase, and those serve as nucleation sites for more energetically favorable crystalline phases [1]. In crystal growth processes, a dense and liquid-like cluster most likely assists formation of a macro-step on a crystal surface [2]. To demonstrate these crystallization processes, *in situ* observation using a microscope is one of the powerful methods because it can directly visualize these processes in real time. However, it is difficult to visualize behavior of such metastable particles because those sizes are normally submicron, sometimes in nanoscale. Recently developed liquid cells adapting to high-vacuum environments of transmission electron microscopy (TEM) provide nanoscale views of nanoparticles and crystallization processes in aqueous solutions [3]. We developed the fluid-reaction transmission electron microscopy (FR-TEM) system for *in situ* observation of crystallization process in aqueous solutions. Using this system, we performed *in situ* observation of a protein crystallization, for investigating its nucleation and crystal growth processes.

Hen-egg white lysozyme was used as a protein sample without further purification and was crystallized using NaCl as a precipitant in a sodium acetate buffer solution at pH = 4.5. For observation of crystals in a solution under TEM, we used a "Poseidon" TEM holder (Protochip, Inc.) combined with a liquid cell. The liquid cell consists of a pair of semiconductor-based plates with an amorphous silicon nitride window and 150 or 500-nm-thick spacer to form a flow path of a crystallization solution.

We succeeded in observing two crystalline phases of orthorhombic and tetragonal in addition to an amorphous phase of the lysozyme [4]. Orthorhombic is the most stable of phases in our experimental solution. In this presentation, we present recent results of *in situ* TEM observation of its crystallization process including behaviors of metastable phases.

### Acknowledgement

The authors acknowledge supports from a Grant-in-Aid for Research Activity Start-up from KAKENHI (26887001), for a grant for Young Scientists (A) from KAKENHI (24684033) and for a grant for Scientific Research (S) from KAKENHI (15H05731).

### References

- [1] M. H. Nielsen *et al.*, *Science* 345 (2014), 1158.
- [2] M. Sleutel & A. E. S. Van Driessche, *Proc. Natl. Acad. Sci. U.S.A* 111 (2014), E546.
- [3] F. M. Ross, *Science* 350 (2015), 6267.
- [4] T. Yamazaki *et al.*, *Microsc. Microanal.* 21 (2015), 255.

Keywords: In situ observation, Transmission electron microscopy, Crystallization, Solution growth, Lysozyme

## Chiral Bias in Chiral Crystallization Induced by Circularly Polarized Laser Trapping of Silver Nanoparticles in Sodium Chlorate Solution

\*Hiromasa Niinomi<sup>1</sup>, Teruki Sugiyama<sup>2</sup>, Miho Tagawa<sup>3</sup>, Kenta Murayama<sup>3</sup>, Shunta Harada<sup>3</sup>, Toru Ujihara<sup>3</sup>

1.Molecular Chirality Research Center, Graduate School of Advanced Integration Science, 2.Applied Chemistry and Institute of Molecular Science, Taiwan National Chiao Tung University, 3.Institute of Materials and Systems for Sustainability, Graduate School of Engineering, Nagoya University

Chiral crystallization, in which chirality emerges spontaneously in the course of crystallization, has been received attention from the viewpoint of emergence of chirality. Thus, the exploration of physical factors that induce a chiral bias in chiral crystallization provides implications for the origin of bihomochirality. Asymmetric interaction between circularly polarized light (CPL) and chiral compound, i.e. circular dichroism (CD), has been considered as a candidate for the origin of bihomochirality,[1]. Many previous studies on photosynthesis of chiral molecule have proven that asymmetric light-matter interaction induces slight chiral bias in enantiomeric ratio of reaction product, so far.[2] However, light-based chiral bias in chiral crystallization still remains unreported. Two conceivable reasons may exist: (1) CD is intrinsically small, (2) there is no investigation on chiral bias by CPL-induced chiral crystallization with a guarantee of optical field effect on nucleation. We overcome these difficulties by two strategies: (1) the plasmonic enhancement of CD [3] and (2) continuous-wave (CW) laser-induced nucleation [4]. In this presentation, we report the first demonstration of significant chiral bias in NaClO<sub>3</sub> chiral crystallization by irradiating a tightly-focused circularly polarized CW laser at the interface between air and a NaClO<sub>3</sub> solution containing plasmonic AgNPs.

A CW CPL green laser (532 nm, 940±5 mW, ellipticity >93%) was focused onto the air-liquid interface of the undersaturated NaClO<sub>3</sub> solution containing AgNPs by using a 60x objective lens (NA = 0.9) equipped on an inverted polarized light microscope. We repeated crystallization and chirality identification of the NaClO<sub>3</sub> crystal 100 times and 100 times by using *l*- and *r*-CPL, respectively. The number of the resulting enantiomorphs was counted.

As the result of the laser irradiation, crystallization occurred from the focal spot. The crystallization using *l*-CPL(*r*-CPL) yielded *l*-enantiomorph 42(65) times and *d*-enantiomorph 58(35) times, respectively, indicating that the *d*-(*l*-)enantiomorph was dominant over the *l*-(*d*-)enantiomorph. Namely, the "dominant" enantiomorph can be switchable by switching the handedness of incident CPL, i.e. the chiral bias is enantioselective. In total, the "dominant" enantiomorph crystallized 123 times out of 200 crystallization. This chiral bias is statistically significant because the number of the "dominant" enantiomorph deviates 99% interval of the binomial distribution  $B(n,p) = B(200,0.5)$ , where  $n$  is the number of trials and  $p$  is the probability that the "dominant" enantiomorph crystallizes out (Figure 1). This deviation demonstrates that the probability  $p$  is more than 0.5, i.e. the probability of the occurrence of each enantiomorph is no longer equal.

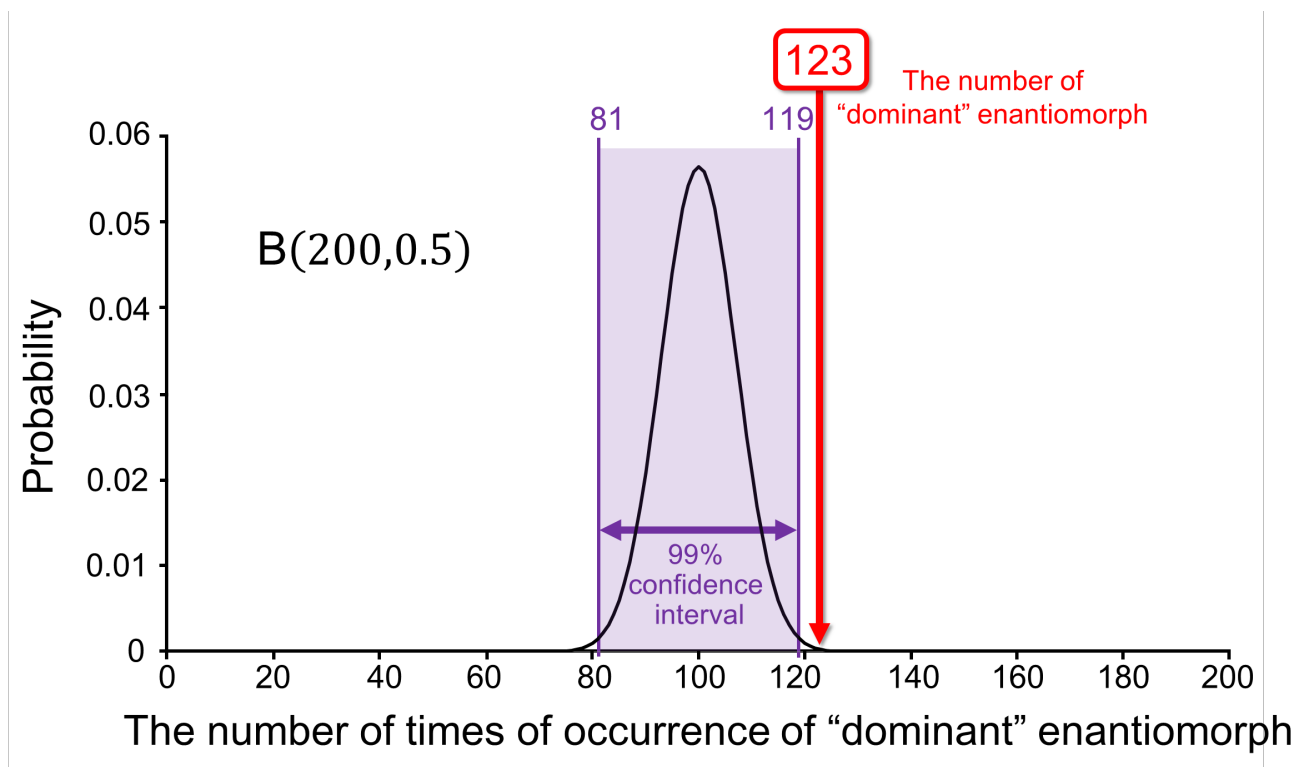
We found that the crystallization of NaClO<sub>3</sub> chiral crystal can be induced by the irradiation of tightly focused CPL laser (532 nm) at the interface between air and NaClO<sub>3</sub> solution containing AgNPs. We also found that this crystallization method can cause a statistically-significant chiral bias in the probability of crystallization of both of the enantiomorphs. Moreover, the "dominant" enantiomorph is found to be switchable by changing the handedness of CPL. Our results may provide implications for the origin of bihomochirality.

[1] W. A. Bonner, *Orig. Life Evol. Biosph.* 21(2), (1991), 59.

[2] B. L. Feringa, R. A. v. Delden, *Angew. Chem. Int. Ed.* 38, (1999), 3418.

- [3] Y. Zhang, C. Gu, A. M. Schwartzberg, S. Chen and J. Z. Zhang, *Phys. Rev. B* 73, (2006), 165405.  
[4] T. Sugiyama, T. Adachi, H. Masuhara, *Chem. Lett.* 36(12), (2007), 1480.

Keywords: chiral crystallization, laser-induced crystallization, circularly polarized light, metal nanoparticle, localized surface plasmon



## Formation of patterns in growth and dissolution of crystals

\*Etsuro Yokoyama<sup>1</sup>

## 1. Computer Centre Gakushuin University

This talk is concerned with fundamental aspects of formation of pattern of crystals in undersaturation. The formation of patterns in crystal growth is a free-boundary problem in which the interface that separates the crystal from an associated solution or vapor phase moves under the influence of non-equilibrium conditions. The formation of patterns in crystal dissolution/evaporation is also a free-boundary problem. The topics of dissolution/evaporation pattern of crystals, however, have been neglected in comparison with the study of growth morphology of crystals except a few studies [1].

The growth patterns depend markedly on conditions in the solution/vapor phase, such as temperature and concentration, which influence the growth speed of each element of the interface. The growth speed of the interface also depends on the local geometry of the interface, specifically on the interface curvature and the orientation of the interface relative to the crystal axes. Although the dissolution/evaporation forms diminish with time, the patterns could also depend on conditions in the solution/vapor phase under the small deviation from equilibrium conditions.

The local motions of interface can, in principle, be determined by solving the transport equations that take into account the following elementary processes:

- 1) a diffusion process for the transport of latent heat liberated or absorbed at the interface,
- 2) a process for diffusing molecules through the solution/vapor phase toward or from the interface, and
- 3) an interface kinetic process for incorporating/decorporation molecules into/from a crystalline phase at the interface[2].

We consider the asymmetry of normal speed at interface relative to the equilibrium point from supersaturation to undersaturation. We shall term the positive normal speed the growth rate of crystallization and the negative normal speed the dissolution/evaporation rate. Both local normal speed  $V$  of the interface can be proportional to the deviation from local equilibrium conditions  $\Delta$ , which depend on interface curvature:

$$V = \beta \Delta,$$

where  $\beta$  is a kinetic coefficient that can depend on interface orientation and the degree of supersaturation or undersaturation at the interface. In general,  $V$  includes the Boltzmann factor  $\exp(-E/kT)$ , where  $E$  is an activation energy,  $k$  is the Boltzmann constant and  $T$  is temperature. Since the factor  $\exp(-E/kT)$  causes enhancement of the dissolution/evaporation rate for  $T > T_e$  but reduction of the growth rate for  $T < T_e$ , the behavior of  $V$  relative to  $T_e$  is asymmetric. On the other hand if  $V$  is controlled by the undersaturation and the factor  $\exp(-E/kT)$  does not work, the dissolution rate can approach a limiting value. This is because the degree of undersaturation has a minimum limit, e.g., pure solvent without solute.

In this talk, we show the patterns during growth or dissolution/evaporation of a two-dimensional crystal under conditions such that the transport of heat and/or solute is so rapid that growth is controlled by interfacial processes. Furthermore, we discuss the formation of both patterns in the point of view of the asymmetry of normal speed at interface relative to the equilibrium point.

## references

- [1] R. Lacmann, W. Franke and R. Heimann, *J. Crystal Growth*, 26(1974)107–116; R. Lacmann, R. Heimann and W. Franke, *J. Crystal Growth*, 26(1974)117–121; W. Franke, R. Heimann and R. Lacmann,

J. Crystal Growth, 26(1974)145-150.

[2] J. P. Hirth and G. M. Pound, J. Chem. Phys., 26(1957)1216-1224; J. P. Hirth and G. M. Pound, Acta Metallurgica, 5(1957)649-653; J. P. Hirth and G. M. Pound, J. Phys. Chem., 64(1960)619-626; J. P. Hirth and G. M. Pound, Condensation and evaporation, Nucleation and Growth kinetics, Progress in Material Science 11, Editor B. Chalmers, Pergamon Press 1963.

## The Coupled Dissolution and Growth

\*Katsuo Tsukamoto<sup>1</sup>

1. Graduate School of Engineering, Osaka University

Lots of discussions on whether growth is an opposite phenomena of dissolution or not. Here after presenting the real rates observed in-situ in both cases at the same absolute value of chemical potential, we show the difference. This may lead to a deeper understanding of coupled dissolution and growth of crystals in solution. We will show even in dissolution process of a crystal crystallization barrier plays an important role.

Keywords: dissolution, growth, mechansim

## Specific Surface Free Energy and Roughening Transition of Sodium Chloride Single Crystal

\*Ryoya Maruyama<sup>1</sup>, Takaomi Suzuki<sup>1</sup>

1. Graduate School of Science and Engineering, Shinshu University

Specific surface free energy (SSFE) is one of important values to discuss the morphology and growth of crystal, and theoretically well discussed. However, experimental trial to determine the SSFE of crystal is very few. We have already measured contact angle of liquids on crystals, for example, apatite, ruby, and quartz in order to determine the SSFE. The SSFE of crystals were proportional to growth rate of crystals, which qualitatively satisfy Wulff's relationship. Experimentally determined SSFE is not that of ideal flat face, but it includes step free energy. This time we tried to measure the step free energy of sodium chloride and discussed the roughness of crystal face.

Sodium chloride single crystal was synthesized by evaporation of saturated water solvent keeping at 40°C. Cubic crystal with (100) face was obtained. Octahedral sodium chloride single crystal with (111) face was also synthesized from water solvent with 15% of formamide keeping also at 40 °C. Crystals was heated by electric furnace at 600°C and kept for 1 hour.

Droplets of ethylene glycol or diethylene glycol with volume of 0.1μL were dropped on the crystal surface using a micropipette. The contact angle were observed using digital camera.

SSFE were calculated by Wu's harmonic mean equation and Fowkes approximation. The calculated value of SSFE of (100) surface before and after heat treatment were 45.9, 48.8mN/m, and SSFE of (111) face before and after heat treatment were 37.9 and 38.9mN/m. The SSFE was increased by heat treatment for (100) and (111) face. Because the observed SSFE contains step free energy, the increase of SSFE is caused by increase of steps on the crystal face. The increase of SSFE was observed after the heat treatment at 600°C. Therefore, the roughening temperature is considered to exist at the temperature under 600°C.

Keywords: specific surface free energy, sodium chloride single crystal, roughening transition

## Surface energy of bubbles evaluated by large-scale molecular dynamics simulations of homogeneous bubble nucleation

\*Kyoko Tanaka<sup>1</sup>, Hidekazu Tanaka<sup>2</sup>, Angelil Raymond<sup>3</sup>, Juerg Diemand<sup>3</sup>

1.Institute of Low Temperature Science, Hokkaido University, 2.Tohoku University, 3.Univ. of Zurich

Bubble nucleation in liquid is a liquid-to-vapor transition phenomenon, and plays an important role in many areas of science and technology. Recently we presented large-scale molecular dynamics simulations of homogeneous bubble (liquid-to-vapor) nucleation with LAMMPS [1]. The simulations contain half a billion Lennard-Jones atoms and cover up to 56 million time steps. The unprecedented size of the simulated volumes allows us to resolve the nucleation and growth of many bubbles per run in simple direct micro-canonical simulations while the ambient pressure and temperature remain almost constant. It is widely believed that classical nucleation theory (CNT) generally underestimates bubble nucleation rates by very large factors. We showed that the measured rates agree well with the CNT within two orders of magnitude in the superheated boiling regime (positive ambient pressure), while the CNT prediction underestimates the nucleation rates significantly in the cavitation regime (lower temperatures and negative pressures) [1,2]. We revisited classical nucleation theory (CNT) for the homogeneous bubble nucleation rate and improve the classical formula using a correct prefactor in the nucleation rate [3]. Most of the previous theoretical studies have used the constant prefactor determined by the bubble growth due to the evaporation process from the bubble surface. However, the growth of bubbles is also regulated by the thermal conduction, the viscosity, and the inertia of liquid motion. These effects can decrease the prefactor significantly, especially when the liquid pressure is much smaller than the equilibrium one. The deviation in the nucleation rate between the improved formula and the CNT can be as large as several orders of magnitude. Our improved, accurate prefactor and recent advances in molecular dynamics simulations and laboratory experiments for argon bubble nucleation enable us to precisely constrain the free energy barrier for bubble nucleation. Tanaka et al. [4] showed that the simple expression including the Tolman correction to the surface tension with a small Tolman length leads to good agreements with the recent MD simulations. But it is also important to compare with other models. The model of surface tension based on the Helfrich expansion is interesting to consider [5], although it includes some additional parameters. Recently, WilhelmSEN et al. [5] obtained values for the parameters in the Helfrich expansion for various temperatures and cutoff radii in the case of a Lennard-Jones liquid using density functional theory (DFT) calculations. The validity of the Helfrich expansion for nanosized bubbles has not yet been fully clarified [5]. We tested the Helfrich expansion model for various bubble sizes and temperatures, using results for surface tension from our MD simulations, and found an agreement stronger than that the pure Tolman description offers.

[1] J. Diemand et al., Phys. Rev. E, 90, 052407 (2014).

[2] R. Angelil et al., Phys. Rev. E, 90, 063301 (2014).

[3] Y. Kagan, Russ. J. Phys. Chem. 34, 42 (1960).

[4] K. K. Tanaka et al., Phys. Rev. E, 92, 022401 (2015).

[5] O. WilhelmSEN et al., J. Chem. Phys. 142, 064706, (2015).

Keywords: bubble nucleation , surface energy , nano particle, molecular dynamics simulation

In-situ IR measurement in homogeneous nucleation process of alumina under  $\mu\text{G}$  environment

\*Shinnosuke Ishizuka<sup>1</sup>, Yuki Kimura<sup>1</sup>, Tomoya Yamazaki<sup>1</sup>, Itsuki Sakon<sup>2</sup>, Yuko Inatomi<sup>3</sup>

1.Institute of Low Temperature Science, Hokkaido University, 2.Graduate School of Science, University of Tokyo, 3.Japan Aerospace Exploration Agency

Homogeneous nucleation process from vapor is characterized by the ratio between time scales for supersaturation increase and for source collision expressed as  $\Lambda$ [1]. Under the physical condition with the same  $\Lambda$  value, homogeneous nucleation process has been regarded to follow the same process. At the dust forming front around evolved stars,  $\Lambda$  value has been calculated to be  $\sim 10^{3-5}$  from total pressure and velocity of stellar wind. In contrast,  $\Lambda$  value of  $\sim 10^{0-2}$  is known for the gas evaporation method which is one of the simplest experimental methods to produce dust analogues via homogeneous nucleation [2, 3].

In-situ IR measurement during nucleation of nanoparticles in the gas evaporation method proved multi-step formation of metal oxide from vapor to crystalline via liquid droplet in our ground based experiment [4]. Using our advanced technique, we measured IR spectra of nucleating alumina and its evolution while nanoparticles are free-flying under  $\mu\text{G}$  environment in which  $\Lambda$  approximates to the value at dust formation region. Specially designed experimental apparatus equipped with dispersive IR spectrometer was loaded to S-520-30 sounding rocket by which the apparatus carried to altitude of 312 km. We also performed ground based experiment combined with FT-IR.

IR spectra of nucleating alumina measured in ground based experiment showed broad absorption extending  $>11 \mu\text{m}$ . Formed nanoparticles were observed by TEM and identified to  $\delta$ -alumina. In contrast, sharp absorption centered at  $13 \mu\text{m}$  was appeared in  $\mu\text{G}$  experiment. This  $13 \mu\text{m}$  band is one of the most indicative features of corundum ( $\alpha$ -alumina) sphere. Corundum is the most plausible candidate for the origin of unidentified  $13 \mu\text{m}$  feature which is often observed for oxygen rich AGB stars with low-mass loss rate [5, 6]. Polymorphic behavior of alumina in homogeneous nucleation process at different  $\Lambda$  will be the key to understand astronomical dust formation.

## Reference

- [1] Yamamoto, T. & Hasegawa, H., 1977 Progress of Theoretical Physics, Vol. 58, No. 3, 816
- [2] Kimura, Y., Miura, H., Tsukamoto, K., Li, C. et al., 2011, J. Cryst. Growth, 316, 196
- [3] Kimura, Y., Tanaka, K. K., Miura, H. & Tsukamoto, K., 2012, Crystal Growth & Design, 12(6), 3278-3284.
- [4] Ishizuka, S., Kimura, Y. & Sakon, I., 2015, The Astrophysical Journal, 803 (2), 88.
- [5] Speck, A. K., Barlow, M. J., Sylvester, R. J. & Hofmeister, A. M., 2000, Astronomy and Astrophysics Supplement Series, 146(3), 437-464.
- [6] Sloan, G. C., Kraemer, K. E., Goebel, J. H. & Price, S. D., 2003, The Astrophysical Journal, 594(1), 483.